Deformation characteristics of aluminium alloys

Authors:

Prof. **Mitar Mišović**, PhD. Met.
University of Montenegro
Faculty of Metallurgy and Technology - Podgorica
mitarm@ac.me

Nebojša Tadić, PhD. Met.
University of Montenegro
Faculty of Metallurgy and Technology - Podgorica
nebojsa@ac.me

Prof. **Duško Lučić**, PhD. CE
University of Montenegro
Faculty of Metallurgy and Technology - Podgorica
dusko.lucic.666@gmail.com

Preliminary note

Mitar Mišović, Nebojša Tadić, Duško Lučić

Deformation characteristics of aluminium alloys

The utilisation of aluminium alloys in structural applications requires knowledge of their characteristics in the elastoplastic area. The deformation of alloys in this area can be described by the Ramberg-Osgood's equation. Tensile test results for AW-5083 and AW-2024 alloys are presented, and it is confirmed that strain hardening can reliably be described with Hollomon equation. Ramberg-Osgood equations are derived for these two alloys based on strain hardening indicators.

Key words:

Aluminium alloys, Hollomon equation, Ramberg-Osgood equation, strengthening factor, strain hardening index

Prethodno priopćenje

Mitar Mišović, Nebojša Tadić, Duško Lučić

Deformacijske karakteristike aluminijskih legura

Primjena aluminijskih legura za građevinske konstrukcije zahtijeva poznavanje njihovih karakteristika u elastičnoplastičnom području. Deformacija legura u tom području može se opisati Ramberg-Osgoodovom jednadžbom. U radu su prikazani rezultati vlačnog ispitivanja legura AW-5083 i AW-2024 i potvrđeno je da Hollomonova jednadžba može pouzdano opisati deformacijsko očvršćivanje. Na temelju pokazatelja deformacijskog očvršćivanja izvedene su Ramberg-Osgoodove jednadžbe za ove dvije legure.

Ključne riječi:

aluminijske legure, Hollomonova jednadžba, Ramberg-Osgoodova jednadžba, koeficijent čvrstoće, indeks deformacijskog očvršćivanja

Vorherige Mitteilung

Mitar Mišović, Nebojša Tadić, Duško Lučić

Deformationseigenschaften von Aluminiumlegierungen

Die Anwendung von Aluminiumlegierungen für Bauwerke setzt die Kenntnis des entsprechenden elasto-plastischen Materialverhaltens voraus. Verformungen von Legierungen in diesem Bereich können mittels Ramberg-Osgood's Gleichung beschrieben werden. In dieser Arbeit werden Resultate von Zugversuchen der Legierungen AW-5083 und AW-2024 dargestellt und es wird bestätigt, dass Hollomon's Gleichung zuverlässig die Verformungsverfestigung beschreiben kann. Aufgrund der Indikatoren zur Verformungsverfestigung werden Ramberg-Osgood's Gleichungen für diese beiden Legierungen hergeleitet.

Schlüsselwörter:

Aluminiumlegierungen, Hollomon's Gleichung, Ramberg-Osgood's Gleichung, Festigkeitskoeffizient, Index der Verformungsverfestigung

1. Introduction

The use of aluminium alloys in structural engineering does not have a long tradition despite the fact that their elastic and yield limits may be greater compared to those exhibited by ordinary structural steel elements. They may potentially be considered as significant construction materials thanks to their favourable properties [1-3]:

- As alloys are corrosion resistant no special protection of structures is needed, which reduces maintenance costs and ensures compliance with requirements in corrosion-prone environments.
- Small weight enables reduction of the overall weight of structures, facilitates transport of assembled units, simplifies the construction work, reduces load imposed on foundations, and lessens the scope of physical work.
- As sections are produced by extrusion, they can be adjusted to achieve minimum weight and desired functionality; this also enables the use of small-size strengthening elements that can easily be connected.

In addition to the above-mentioned properties, the following features also contribute to the safety of structures:

- resistance to brittle fracture (in the low temperature range), small susceptibility to temperature gradient and residual stress;
- resistance to impacts (positive influence of the speed of deformation on the strength and ductility);
- plentiful solutions and modern technologies for the connection of elements.

Aluminium alloys can advantageously be used in structural applications when full use is made of one of the three above mentioned key properties: corrosion resistance (C), small weight (L), and functionality of cross-section (F). Numerous examples of such structures are given in papers presented by Mazzolani, Kissell, Lundiberg, Dwigth [1-4], and in publications specialized for aluminium [5-8]:

- long truss girders and roof systems in which variable loads are small in comparison with self-weight;
- structures at inaccessible sites, far away from transport routes, where low-cost transport and easy assembly are of great significance (overhead line supports, staircases, temporary bridges);

- structures affected by corrosion and moisture (roof structures of swimming pools, bridges, water engineering facilities, and offshore structures);
- structures with moveable elements, so that servicing is easy and economical (mobile bridges for pedestrians and motor vehicles, rotary bridge cranes at round pools in wastewater purification plants);
- special purpose structures where maintenance is extremely difficult and where weight must be limited (masts, lighting towers, motorway portals, traffic signs).

Although not all of the mentioned cases are related solely to civil engineering, it is clear that the use of aluminium alloys in civil engineering is sustainable [9], and that the scope of possible applications is widening, especially in the areas of modern and less traditional applications [10]. Figure 1 shows typical truss structures made of aluminium alloys. Advantages of the (F + L) criteria are primarily used in case of truss structures, while advantages of the (C) criterion are also often used.

The sequence in which aluminium structures are designed differs from that used for steel structures. Thus, in case of aluminium structures, the design starts by checking allowable deflection, which is followed by verification of the stress and capacity of structural elements [11, 12]. The deflection of the aluminium element's cross section can be verified by harmonizing it with the deflection of a steel element. The following equation is used:

$$\frac{5ql^4}{384\,I_{\check{C}}\,E_{\check{C}}} = \frac{5ql^4}{384\,I_{Al}\,E_{Al}} \tag{1}$$

where:

$E_{\check{C}}, E_{Al}$ - elastic moduli of steel and aluminium
$I_{\check{C}}, I_{Al}$ - moments of inertia of steel and aluminium
q - load
l - span of the structure.

As the relationship $E_{\check{C}} \approx 3E_{Al}$ applies to the moduli of elasticity for the same load and span, the relationship of the moments of inertia at cross-section has to meet the following requirement:

$$I_{Al} \approx 3I_{\check{C}} \tag{2}$$

The strength and plasticity characteristics in the elastic-plastic area of load must be known to enable determination of critical

Figure 1. Examples of truss structures made of aluminium alloys [4, 7]

stresses and safety factors for aluminium alloy structures. The analytical dependence used for describing deformation behaviour in this area is the Ramberg-Osgood equation. This empirical non-linear equation links the elastic modulus and strain hardening indicators with an overall deformation [13]. At static load, the following equation is used:

$$\varepsilon = \frac{\sigma_e}{E} + \left(\frac{\sigma_R}{K}\right)^{\frac{1}{n}}$$
(3)

where:
ε - strain,
σ_e - stress at elastic limit
σ_R - real stress
E - modulus of elasticity
K - strength coefficient
n - strain hardening exponent.

In the case of cyclic loading, the influence of the number of cycles should also be taken into account, as shown in the Manson-Coffin equation [14]:

$$\varepsilon = \frac{\sigma_f'}{E}(2N)^b + \varepsilon_f'(2N)^c$$
(4)

where:
ε - strain,
σ_f' - fatigue strength coefficient
N - number of cycles
ε_f' - fatigue ductility coefficient
b - fatigue strength exponent
c - fatigue ductility exponent.

Strain hardening, fatigue strength, and ductility exponents are linked with the following relationship [14]:

$$n = \frac{b}{c}$$
(5)

while the strength, fatigue, and ductility coefficients are linked as follows:

$$K = \frac{\sigma_f'}{\varepsilon_f'^{b/c}}$$
(6)

At relaxation of load, the elastic-plastic behaviour of material results in deviation from the initial behaviour of material due to mechanical hysteresis. The deformation behaviour based on the Ramberg-Osgood equation for aluminium structures is specified

in EN 1999-1-1 (Appendix E) [15]. The research conducted in this area is now very topical as the nonlinear dependence between the stress and plastic deformation requires laboratory testing, numerical modelling, and design adapted to real strain hardening [16]. Reliable models (equations) enable simulation of behaviour of structural elements based on the finite-element method (FEM) [17]. As the parameters given in equation (3) can be analysed as a function of temperature, it is also possible to analyse the influence of fire hazard on the behaviour of alloys and structures [18]. Knowledge of the influence of temperature on deformation behaviour is also a precondition for defining stability zone of welded structures [19], and requires harmonization of coefficients given in the Ramberg-Osgood equation with real properties of welded connections [20]. This is also valid for the fracture toughness properties, when these properties are a prerequisite for the use of aluminium alloys [21].

Tensile or tensile/compressive stresses (for cyclic loads) are used for laboratory testing [13, 14], although the verification of strain equation correction with spherical indentation device [22] can also be applied.

Results obtained by experimental testing of deformation characteristics of aluminium alloys are presented in this paper. Two alloys belonging to two distinct aluminium alloy groups, both widely used in various structures, were selected: thermally hardening alloys and thermally non-hardening alloys. The deformation behaviour of samples during tensile tests was monitored for two alloy conditions (soft-annealed and hard-deformed). Diagrams with measurement results were analysed from the aspect of specific features related to deformation ageing and accuracy of stress values (technical yield limit in particular) for the experimental procedure applied. Numerical processing involved the use of Hollomon equation for the change of stress as related to the level of deformation. Thanks to reliability of this non-linear equation in the plastic deformation interval, it was possible to define appropriate coefficients in the Ramberg-Osgood equation. Experimentally defined and calculated values were compared with data from relevant literature.

2. Experimental part

2.1. Materials and testing procedure

The alloys AW-5083 and AW-2024 were tested. Their chemical composition is presented in Table 1.

Table 1. Chemical composition of alloys AW-2024 and AW-5083

Alloy designation	Content of alloying elements[1], [%]								
	Cu	Mg	Mn	Si	Fe	Zn	Cr	Ti	Al
AW-5083	0.015	4.23	0.42	0.13	0.26	0.02	–	–	Balance
AW-2024	4.8	1.41	0.42	0.13	0.28	0.07	≤0.01	0.015	
[1] The content of alloying elements is compliant with: International Alloy Designations and Chemical Composition Limits For Wrought Aluminum and Wrought Aluminum Alloys, The Aluminum Association Inc., 2009.									

The alloy AW-5083 belongs to the Al-Mg-Mn system. Thanks to good solubility of magnesium (Mg) in the hard solution of aluminium, the alloy has a pronounced capability of hardening through alloying and deformation, a good strength and ductility ratio, great capability of shaping in complex operations, corrosion resistance, and good weldability. Considering the fact that it does not harden through thermal action, it does not involve tempering when processed to final dimensions and properties, and so it retains a high accuracy of dimensions. Although alloying with magnesium enables achievement of high strength while not greatly reducing the plasticity, the content of about 4.5 % of Mg offers an appropriate hardening relationship through alloying and deformation. Manganese (Mn) exerts a primary influence on the recovery and recrystallization processes, and hence on the control of the size of metal grains, anisotropy of properties and texture.

The plasticity of alloys enables preparation of all kinds of semi-manufactured products (bars, sheet metals, wires, sections, forged pieces) using hot and cold processing procedures. Semi-manufactured products can easily be cold formed by conventional methods. Alloys are characterized by a very good weldability.

The alloy AW- 5083 is most often used in the manufacture of boats and other means of transport, welded pressure cookers, marinas, television towers, military missile components, and many other parts in various fields.

The alloy AW-2024 belongs to the Al-Cu-Mg-Mn system. The main alloying element is copper (Cu) (up to 4.9 %). Thanks to the change in its solubility in aluminium with the change of temperature, the material causes hardening by precipitation and so the alloy achieves high strength and satisfactory ductility. Because of such favourable properties it has long been in use (Alcoa produces it since 1931). The same group includes alloys AW-2124 and AW-2324, as well as alloys characterized by higher purity (smaller iron and silicon content), which results in a more favourable fracture toughness. An additional improvement of properties of these alloys involved a special protection against corrosion. This resulted in development of *Alclad* conditions in which a thin coat of pure aluminium is applied on the surface (nominal thickness of this aluminium coat amounts to 5 % of thickness for sheet metals up to 1.57 mm in thickness, or 2.5 % for sheet metals of more than 1.57 mm in thickness [23]).

The alloy is finally prepared in annealed (0) and thermally hardened conditions (T3, T4, and T8) [24, 25]. It is suitable for further processing and so it is used for the manufacture of all types of semi-manufactured products which, in the annealed conditions, are suitable for final cold forming.

Welding can be conducted using either the resistant welding or electric arc welding procedure in protected atmosphere. Welding by any procedure causes pronounced deterioration of corrosion resistance in the weld zone, which is why welded connections must be subjected to subsequent thermal processing.

Mechanical processing in the thermally processed and annealed condition is favourable.

The alloy is most often used in the production of airplane parts, elements of other means of transport, bridge elements, instruments, various machine parts, and connection elements. AW-5083 alloy samples were made of the rolled strip 1.28 mm in initial thickness, which was cold rolled to 1 mm. The industrially rolled strip 5 mm in initial thickness was used for the alloy AW-2024. This strip was then processed to 2 mm in thickness by rolling using the laboratory rolling machine, and by annealing according to the plan shown in Figure 2. The annealing of samples was completed in the laboratory oven with the temperature regulation accuracy of ±2°C. The deformation hardened condition of alloys was obtained by cold rolling with 20% reduction in thickness. Annealed and deformed conditions were marked with 0 and H, respectively.
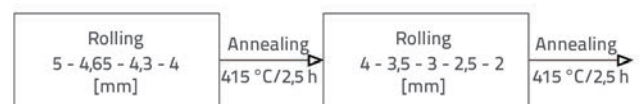
Figure 2. Cold rolling / annealing of AW-2024 alloy strips

The tensile testing was performed using the universal electronic apparatus for testing mechanical properties of materials, type HACKERT FPZ 100/1. The apparatus can conduct tensile, compressive, shearing and bending tests for forces ranging from 20 N to 100 kN. Force measurement signals and sample size changes can be either registered on paper or recorded electronically. The measuring scale (increase) for registration of signals can be adapted to the selected sample, alloy and condition.

3. Test results and analysis

3.1. Tensile strain

Experimental force (F) – extension (Δl) diagrams for the annealed and deformed alloy AW-5083 samples are presented in Figure 3. Typical extension values for which the force value was registered are shown by means of lines parallel to the initial elastic part of the diagram (Figures 3.a and 3.b). These diagrams are then translated into the stress-strain values, based on which the processing and analysis of results was made. Tested samples are of standard form and size. The sample measurement length (l_o) was adapted to the metal sheet thickness (Figure 3.c) [26].

In both cases, the change in force value shows the alloy's pronounced strain deformation capability with a different effect for both conditions. The change of diagram for the annealed and deformed condition can be seen in force values for the uniform and total extension. In addition, force variations are highly pronounced for the annealed condition in most parts of the diagram (alternating vibration around the average value). The variation starts once a certain final deformation is achieved, and is present in case of the aluminium alloy deformation by
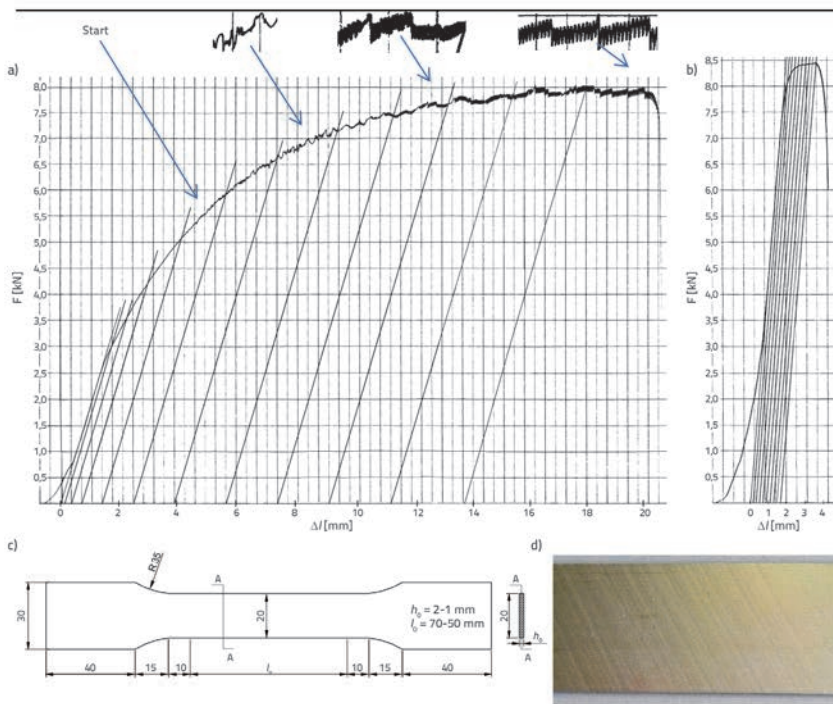
Figure 3. a) Experimental force-extension diagrams for the alloy AW-5083; b) for the annealed cold rolled condition with 20 % reduction in thickness; c) standard form of samples for testing mechanical properties by extension; d) view of the flow strips on the surface of polished samples tested in annealed condition

The occurrence of an uniform increase and reduction of force is called the discontinuous yield or the Portevin – Le Chatelier effect. This occurrence is described by several models. The Cottrell model is based on the relationship between the velocity of dissolved alloying atoms and the dislocation. In case when the concentration of dissolved atoms around the dislocation becomes sufficient, the dislocation is blocked. The number of mobile dislocations decreases suddenly, which causes an increase in strain. When the strain attains the value enabling liberation or activation of blocked dislocations by multiplication mechanism, the number of mobile dislocations increases and the strain reduces. The alternating increase and reduction of strain causes discontinuity on the hardening line, which is analogous to the strain ageing. As dissolved atoms are in interaction with mobile dislocations, this phenomenon is called the dynamic strain ageing [27].

The discontinuity phenomenon is also accompanied by macroscopic manifestation of the dynamic strain ageing, which is visible along the flow strips regularly distributed on the polished sample surface (Figure 3.d).

tension, compression and torsion in a specific temperature and deformation rate interval. The form and amplitude of variation are characteristic for individual degrees of deformation (separately presented in Figure 3.a). In the area of smaller deformations they are limited, in the area of intermediate deformations the cycle amplitude and the number of cycles increase during deformation, and in the area of high plastic deformation, the process is approximately stationary for the number of cycles and amplitude size.

Cold rolling of sheet metal with the 20 % reduction in thickness causes the deformation hardening (transition from the 0 condition to H condition). The number of dislocations is greatly increased in the process. That is why a much greater strain is required as from the start of tensile deformation of samples, and reactions between dislocations (dislocation noises and tangles) are dominant compared to reactions with dissolved
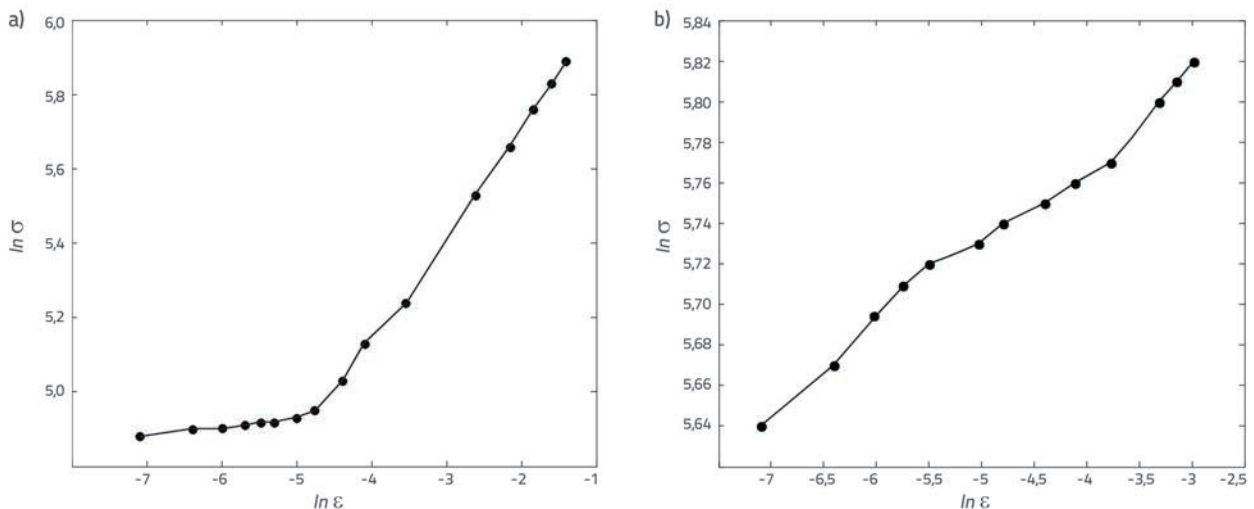
Figure 4. Dependence of results $ln\sigma = f(ln\varepsilon)$ of the alloy AW-5083: a) for the annealed condition; b) deformed condition

alloying atoms. The alternating variation of stress values cannot be observed in the diagram, and the plastic area decreases significantly (Figure 3.b).

The results taken from the diagram were used to calculate the values of relative deformation by extension (ε) and real stress (σ) using the following formula:

$$\varepsilon = \frac{\Delta l}{l_0}; \quad \sigma = \frac{F}{A_0}(1+\varepsilon) \tag{7}$$

where:

F - tensile force
A_0 - initial cross-section of the testsample
Δl - extension (length increase in test sample by elongation)
l_0 - initial measurement length in test sample.

Figure 4 shows the alloy AW-5083 results presented in the logarithmic coordinate system. Two areas with different strain hardening coefficients can clearly be seen for the annealed condition (Figure 4.a). This form is known as the "2n" strain hardening [28]. The strain condition has practically a uniform shape throughout the plasticity interval (Figure 4.b).

The results obtained for the alloy AW-2024 are analogous to the results presented in Figures 3 and 4.

3.2. Accuracy of measurement results

Positions on the force-extension diagram (Figure 3) can accurately be determined down to 0.5 mm. In case of extensions with regard to the measurement range of a standard test tube, this accuracy corresponds to the relative strain of $\varepsilon = \pm0.0005$, which is at the same time the first value registered in the plastic deformation range. In case of force, the accuracy of 0.5 mm implies the error of $\pm$ 20 N, i.e. the stress calculation error of approximately $\pm$ 0.6 N/mm². As the registration accuracy is satisfactory in both cases, all force and extension results were read from the shape diagram presented in Figure 3.

The dispersion of values in case when a greater number of samples is tested is especially significant with regard to the work objective set in advance. In order to reduce this dispersion, all test samples were made of the same narrow strip cut from the sheet metal in the direction of length (rolling direction). The strips were accurately rolled to the measurement thickness using the laboratory rolling machine. In this way the influence of "history" on mechanical properties was reduced to minimum. As a result, stress deviations from the mean value amounted to ±20 MPa for 3-5 samples. It can be noted for comparison purposes that, in case of dynamic ageing, the variation causes stress differences of up to ±8 MPa.

3.3. Analytic processing of results

The strain hardening of aluminium alloys (in 0, T, and H conditions) can be approximated with the Hollomon equation of shape:

$$\sigma = K\varepsilon^n \tag{8}$$

Table 2. Equations and statistical indicators describing strain hardening of alloys tested

Condition	Strain area	Coefficients		Equation	No.	Correlation indicators	
		lnK	n			r-coefficient[1]	s_{est}-error[2]
Alloy: AW-5083							
0	0 - 0.2483	6.0550	0.2004	$\sigma = 426.23\varepsilon^{0.2004}$		0.9548	0.1178
	0 - 0.0086[3]	5.0441	0.0231	$\sigma = 155.09\varepsilon^{0.0231}$	(9)	0.9809	0.0036
	0.0086 - 0.2483	6.2723	0.2816	$\sigma = 529.67\varepsilon^{0.2816}$	(10)	0.9988	0.0192
H	0 - 0.0509	5.9296	0.0396	$\sigma = 375.99\varepsilon^{0.0396}$	(11)	0.9903	0.0071
Alloy: AW-2024							
0	0 - 0.1968	5.9513	0.2372	$\sigma = 384.27\varepsilon^{0.2372}$		0.9876	0.0742
	0 - 0.0026[3]	4.8306	0.0627	$\sigma = 125.28\varepsilon^{0.0627}$	(12)	0.9795	0.0096
	0.0026 - 0.1968	6.0457	0.2672	$\sigma = 422.28\varepsilon^{0.2672}$	(13)	0.9989	0.0202
H	0 - 0.0235	5.7296	0.0328	$\sigma = 307.85\varepsilon^{0.0328}$	(14)	0.9768	0.0070

[1] Pearson correlation coefficient for n pairs of linear dependence $X = ln(\varepsilon)$ and $Y = ln(\sigma)$ is:

$$r = \frac{n\Sigma XY - \Sigma X \Sigma Y}{\sqrt{n\Sigma X^2 - (\Sigma X)^2}\sqrt{n\Sigma Y^2 - (\Sigma Y)^2}}$$

[2] Standard approximation error according to the derived linear dependence equation $X = ln(\varepsilon)$ and $Y = ln(\sigma)$ is:

$$s_{est} = \sqrt{\frac{\Sigma(Y-Y')^2}{N-2}}$$

[3] Strain areas are calculated based on the straight line intersection points for the first and second strain hardening intervals

Table 3. Comparison of measured and calculated strain values for the alloy AW-2024

Measured values				Calculated values		Stress difference $\sigma_p - \sigma_m$ [MPa]	Strain hardening $\Delta\sigma = \sigma_p - \sigma_{0,01}$ [MPa]
Strain		Force F [N]	Stress σ_m [MPa]	Exponent n	Stress σ_p [MPa]		
Δl [mm]	ε						
	0.0001				72.01		
0.5	0.0005	2750.0	77.95		77.83	-0.13	
1.0	0.0010	2850.0	80.83	0.0627	81.38	0.55	12.99
1.5	0.0015	2931.3	83.18		83.39	0.21	
2.0	0.0021	3006.3	85.35		85.00	-0.35	
2.5	0.0025	3146.9	89.39		85.59	-3.79	
3.0	0.0031	3234.4	91.92		90.21	-1.72	
4.0	0.0041	3403.1	96.82		97.31	0.49	
5.0	0.0053	3562.5	101.47		104.10	2.63	
7.5	0.0077	3937.5	112.42		114.98	2.56	
10.0	0.0104	4225.0	120.94		124.53	3.58	
19.5	0.0202	5096.9	147.33	0.2672	148.94	1.61	201.48
35.0	0.0356	5934.4	174.12		173.16	-0.95	
55.0	0.0555	6650.0	198.87		195.01	-3.85	
79.5	0.0806	7165.6	219.37		215.43	-3.94	
105.0	0.1057	7462.5	233.78		231.65	-2.13	
129.5	0.1308	7701.9	246.75		245.20	-1.55	
159.5	0.1610	7809.4	256.87		259.20	2.32	
194.0	0.1968	7990.6	270.94		273.49	2.55	

The coefficients K i n are analogous to the coefficients defined in equation (3).

Although other equations have also been developed, the Hollomon equation contains the coefficients K and n that can accurately be defined thanks to an appropriate physical significance. The strength coefficient K corresponds to the strength (stress: σ) at which the strain value (ε) is equal to one (based on equation (7), this means that an increase in sample length Δl has reached an initial measurement length l_0). The strain hardening exponent n is the strain hardening rate. In logarithmic coordinates this equation is translated into a straight line with the section at s-axis equalling to lnK, and with inclination amounting to $tg\alpha = \Delta\sigma / \Delta\varepsilon = n$ (Figure 4).

Consequently, all experimental data were translated to the logarithmic coordinate system (linear function) and then the K and n values were determined by the least-squares method. The software STATGRAPHICS CENTURION (freely available in test version) was used [29]. The program enables automatic data processing in linear form with the calculation of coefficients, reliability criteria indicators, and with graphical presentation of diagrams and reliability intervals. The program enables selection of a number of functions (equations) that are checked and ranked based on the functional dependence method selected, and according to statistical approximation indicators obtained. In this particular case, the least squares method was used. Some

other equations that the program package can verify were also tested in parallel with the Hollomon equation. The following indicators were monitored: correlation coefficient r, significance level p, and standard correlation error s_{est}. In the results, the program shows all equations in which these indicators are favourable or close to the desired linear equation [29]. K and n values, statistical indicators and the corresponding equations are shown in Table 2. The lowest correlation coefficient for linear dependence should amount to $r > 0.95$, in order to confirm the relatively reliable dependence between the variables. In the analysis of variance (abbreviated as: (ANOVA) the empirical p-value should amount to $p < 0.05$, in order to confirm the significance of dependence in the 95% standard confidence interval. The standard correlation error s_{est} shows the expected deviation of design values using the derived equations for the prediction of results [29].

Statistical parameter results presented in Table 2 show that the strain hardening of alloys can reliably be approximated in both conditions by means of the Hollomon equation. The values K and n differ sufficiently for each testing condition, and so their use requires prior knowledge of the data about the accurately selected alloy and condition.

The lowest correlation coefficient value for the alloy AW-5083 was obtained in the annealed condition (0.955). Although the coefficient is greater than 0.95 (p value is smaller than 0.05) and
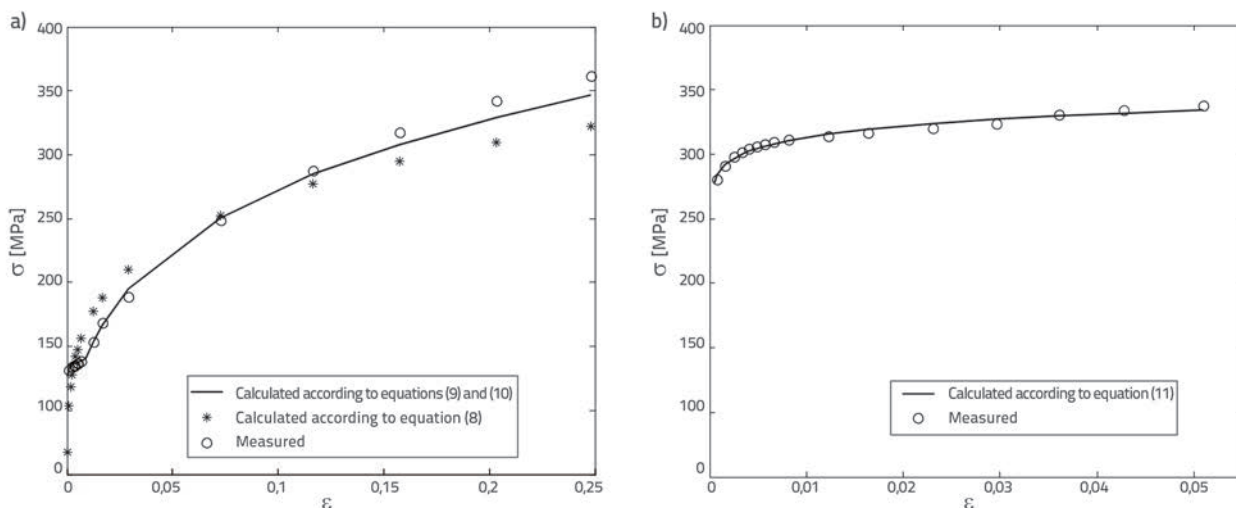
Figure 5. Comparison of results for the measured and calculated σ - ε diagram values for the alloy AW-5083: a) in annealed condition; b) in deformed condition

the correlation can thus be considered satisfactory, the form of the diagram presented in Figure 4.a points to the obvious presence of two strain behaviour areas. That is why the equation determination procedure with the division in two intervals was used. An additional reason for this division is the fact that a special significance is accorded to the first interval because it covers both the elastic limit and the technical yield limit.

By dividing the strain hardening into two intervals, the correlation coefficient is improved in both intervals and it attains high values (0.981 and 0.999), while approximation errors are reduced significantly.

The correlation coefficient for the deformed condition amounts to 0.990, which means that the entire plastic behaviour interval can be approximated with a single equation.

Measured and calculated values for the alloy AW-2024 are presented in parallel in Table 3, while the corresponding values for the alloy AW-5083 are given in Figure 5.

In the annealed condition of the alloy AW-2024, the correlation for the first interval is slightly reduced (from 0.988 to 0.979) by division of areas into intervals, but the approximation error is also greatly reduced. The correlation coefficient for the second area is high and amounts to 0.999. This is also confirmed by the differences between the calculated and measured stress values σ_p - σ_m) presented in Table 3. This justifies the use of two intervals in this alloy as well. Here also the correlation coefficient is high for the deformed condition and it amounts to 0.978. Thus the use of a single interval and equation is considered justified.

Figure 5 Comparison of results for the measured and calculated σ - ε diagram values for the alloy AW-5083 a) in annealed condition; b) in deformed condition

In this way, statistical interpolation indicators confirm beyond doubt that the Hollomon equation (8) can reliably be used for the description of strain behaviour of the tested alloys and their conditions. It is significant to note that separate equations (11) and (14) with a high correlation coefficient can be used in case

of deformed condition, while partial equations (9), (10), (12), and (13) must be used in case of annealed condition. In accordance with the objective set for this paper, these equations will be used for the determination of limit states, for derivation of the Ramberg-Osgood equation for total strain, and also for identification of the capacity of alloys to harden by deformation, which is also significant for the behaviour of materials and for the bearing capacity of structures.

3.4. Limit strain values

The use of plane samples (Figure 3.c) for the characterisation of materials is rendered additionally complex due to different values of properties in the plane and along the metal thickness, and to anisotropy of properties in the metal plane, depending on the direction of testing. In this paper, the testing was conducted solely along the length of samples, i.e. in the sheet metal rolling direction. If the aim is to characterise anisotropy then it would be necessary to apply the same procedure to other directions (most often $\pi/4$ and $\pi/2$ with respect to the direction of rolling). Experimental determination of the proportionality limit (σ_p) was not made as it can not accurately be defined using the existing strain change test (10 % deviation from linear dependence of the force-extension diagram is required). Also, the elastic modulus can not accurately be determined using this procedure [30], and so the corresponding data were taken from appropriate standards (Table 4).

It also proved impossible to determine the technical elastic limit (σ_e) by experiment as the first reliably registered strain value was much higher than the permanent strain specified in the standard (e=0.01 %). That is why the elastic limit was determined based on equations given in Table 2. The obtained results are given in Table 4.

The technical yield limit ($\sigma_{0,2}$) for materials characterized by this diagram is determined for the permanent strain of 0.2 %. The

Table 4. Data for elastic modulus and limit stress of alloys under study

Alloy	Condition	Measured	Calculated	Literature data [23, 31-33]
		Elastic modulus [GPa]		
AW-5083	0, H	-	-	71
AW-2024	0, H	-	-	73
		Technical limit of elasticity (ε = 0,0001)[1] [MPa]		
AW-5083	0	-	125.37	-
	H	-	261.08	-
AW-2024	0	-	70.32	-
	H	-	227.58	-
		Technical limit of yield (ε = 0,002)[1] [MPa]		
AW-5083	0	134.72	134.08	min 125
	H	290.64	293.38	min 250
AW-2024	0	81.75	84.68	max 96
	H	253.39	250.58	-
		Tensile strenght[1] [MPa]		
AW-5083	0	289.66	286.62	min 275
	H	318.54	317.98	min 305
AW-2024	0	222.94	228.53	max 220
	H	266.12	265.96	-

[1] Limit stress values are determined with regard to the initial cross-section area and can be calculated from the real stress using the expression $\sigma/(1+\varepsilon)$

		Strain hardening as related to technical limit of elasticity							
Alloy	Condition	Until the limit of 0,2 %		Until the limit of 3,5 ‰		Until the limit of 10 ‰		Until the tensile strength	
		[MPa]	[%]	[MPa]	[%]	[MPa]	[%]	[MPa]	[%]
AW-5083	0	9	7	11	9	19	16	232	185
	H	33	13	39	15	52	20	73	28
AW-2024	0	15	21	23	33	53	75	201	289
	H	23	10	28	12	37	16	45	20

Table 5. Ramberg-Osgood equations for alloys under study

Alloy	Condition	Equation	No.	Stress range [MPa]	Proportion of strain %ε_{el}/ %ε_{pl}	
					At technical limit of elasticity	At technical limit of yield
AW-5083	0	$\varepsilon = 0.00177 + (0.00645\sigma)^{43.29}$	(15)	< 139	95/5	28/72
		$\varepsilon = 0.00177 + (0.00189\sigma)^{3.55}$	(16)	140-356		
	H	$\varepsilon = 0.00369 + (0.002669\sigma)^{25.25}$	(17)	< 334	97/3	61/39
AW-2024	0	$\varepsilon = 0.00096 + (0.00799\sigma)^{15.95}$	(18)	< 86	95/5	19/81
		$\varepsilon = 0.00096 + (0.00237\sigma)^{3.74}$	(19)	86-274		
	H	$\varepsilon = 0.00313 + (0.00325\sigma)^{30.49}$	(20)	< 272	97/3	65/35

technical yield limit () is included in all tests for the guaranteed mechanical properties. The $\sigma_{0,2}$ data determined experimentally and calculated according to equations form Table 2 are presented in Table 4. Literature data (according to standard values, i.e. according to values guaranteed by selected manufacturers) are also presented for comparison purposes. As the first interval for the annealed state is related to plastic area comprising the

technical yield limit, the calculation of stress was completed for this limit condition according to equations (9) and (12).
The tensile strength results (σ_u) were determined based on limit values of stable plastic deformation.
The data given in Table 4 show that some limit stress values are fully harmonised with the data given in the standard. The presented procedure for analytic determination of elastic and plastic limit
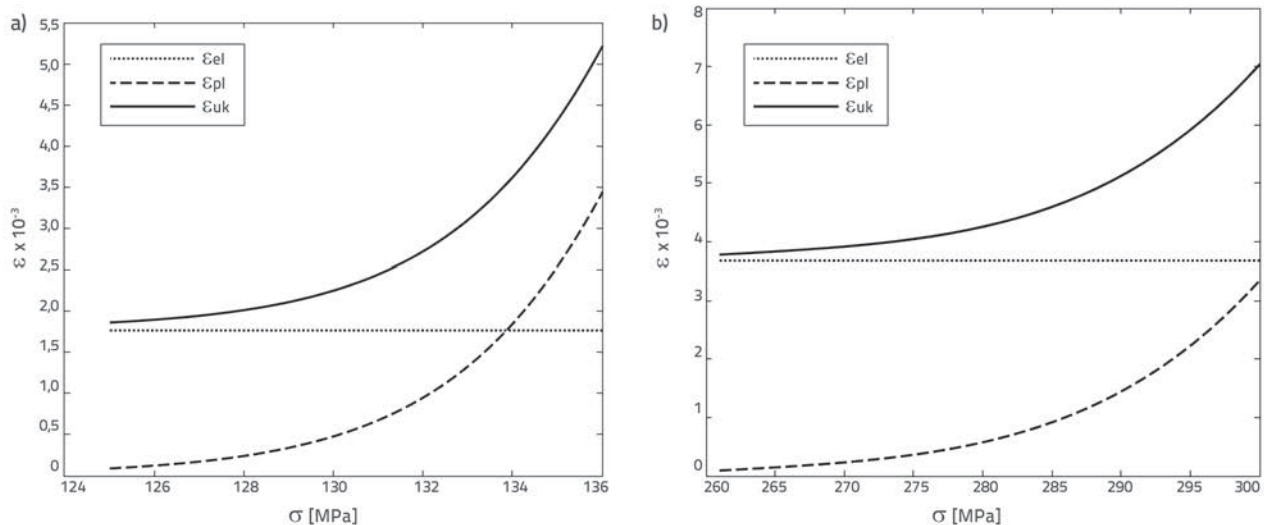
Figure 6. Dependence of elastic, plastic and total strain on stress, for alloy AW-5083 in: a) annealed condition; b) deformed condition

is highly reliable as the correlation coefficient values are high, and the approximation error for experimental data, with relevant equations, is practically within the measurement error limits. A good correspondence between the measured and calculated values was established, as shown in Table 3 and Figure 5.

Strain hardening in the zone between the limit stress values (Table 4) shows to what extent stress must be continuously increased to reach the required strain, i.e. to make the material pass from one limit state to another. Various hardening values were registered for the alloys under study. It should however be noted that, in the first interval, from the technical limit of elasticity to the technical limit of yield, the alloys harden by 7 to 21 % compared to the stress at the technical limit of elasticity, which is a significant increase in a highly restricted plastic area. Table 4 gives a parallel presentation of hardening up to the limit of 3.5 ‰, which corresponds to the limit plastic deformation of concrete, and 10‰, which corresponds to the Lüders extension of the ordinary structural steel (horizontal part of the diagram once the lower yield limit is achieved). Hardening of analysed alloys for the defined limit deformation of concrete varies from 9 % to 33 %, and for the defined limit deformation of steel it can achieve 71 % (in the same interval, strain hardening is negligible in case of ordinary structural steel). Continuous strain hardening, which follows the load action, has a positive effect as it causes an increase in stress values in the zone of a very limited plastic deformation. This increase is particularly significant in the zone between the technical limit of elastic yield, as it may suggest that any plastic deformation due to changeable and/or extraordinary load will be manifested locally, and that it will cause an increase in limit stress of the alloy and increase in safety factors in the interval until the above mentioned strain hardening values are reached.

Ramberg-Osgood equations were derived for the alloys under study based on the results obtained for the technical limit of elasticity (σ_e), elastic modulus (E), strength coefficient (K), and the strain hardening exponent (n). These equations are presented in Table 5, in parallel with stress zones in which they

can be used, and with the relationship between elastic and plastic strain proportions at the technical limit of elasticity and yield. Diagrams of change in elastic, plastic and total strains in the zones up to the limit of 3.5 ‰ are presented in Figure 6 for the alloy AW-5083.

The values of all coefficients in equations are sufficiently different from each other and so their use has to be adapted to the selected alloy and condition. The first term in equations (15) to (20) is the elastic strain value. For a constant stress value, it can be programmed using alloy hardening procedures because elastic modulus (as a physical characteristic of material) is practically independent from these procedures. For the elastic range until the technical limit of elasticity, the proportion of elastic strain is 95-97 %. The proportion at technical yield limit depends on initial conditions: with prior strain hardening the alloy is maintained at the level of > 60 %, while the proportion is much lower in the annealed (soft) condition.

When the equation coefficient values are dependent on the initial condition (property), their differences may be expected in all cases when the conditions exert changes to initial properties of alloys. This has also been confirmed by the experimental study of deformation behaviour of welded connections made of the alloy AW-5083, presented in [20]. The values of $\sigma_{0,2}$ = 161 MPa and n = 0.142 (1/ n ≈ 7) were obtained for the basic alloy. The difference in $\sigma_{0,2}$ and $1/n$, as related to the data given in Table 4 and equation (15), can be a consequence of mechanical and thermal treatment, but may also be due to the experimental measurement procedure used. The same may also be valid for the difference in the annealed condition as related to the values of $1/n$ = 10-20 for non-hardened alloys recommended in paper [13] (the data were obtained based on forms presented in EN 1999-1-1). In the same paper, and also in paper [34], the value of $1/n$ = 20-40 is recommended for hardened alloys. Although coefficients given in equations (17) and (20) correspond to this recommendation, the intervals for these two alloy groups are

relatively wide and can be used for information only. Considering the significance of equations, the described procedure of exact analytic processing and determination of limit stress values, strength coefficient, and strain hardening exponents based on Hollomon equation, can be considered as fully justified.

4. Conclusion

The analyses presented in this paper are aimed at studying deformation behaviour of aluminium alloys under the influence of tensile stresses. Initial experimental curves are obtained by tensile testing of standard sheet metal samples for the alloys AW-5083 and AW-2024. In the analysis of experimental results, the authors explain typical changes, present the analytical processing procedure, and derive equations that are needed to describe deformation characteristics.

Based on the results and analyses, it was confirmed that the strain hardening of the studied alloys can reliably be approximated with Hollomon equation. At that, two hardening zones were accurately identified for the annealed conditions.

This separation of zones is significant because the first zone contains technical limits of elasticity and yield, which are used for determining the bearing capacity of structures.

The analytic description of strain changes has enabled derivation of Ramberg-Osgood equations, which consistently link the elastic and plastic areas, based on their exact connection with strain hardening properties for the tested alloys and conditions. High correlation coefficients for the derived analytic dependencies and simple procedure suggest that this procedure can also be used for the study of other aluminium alloys.

Acknowledgements

REFERENCES

[1] Dwight, J.: Aluminium Design and Construction, Taylor & Francis Group, 1999., http://dx.doi.org/10.4324/9780203028193

[2] Kissell, J.R., Ferry, R.L.: Aluminium Structures - A Guide to Their Specifications and Design, Second Edition, John Wiley & Sons, 2002, pp. 337-423.

[3] Mazzolani, F.M.: Design Criteria for Aluminium structures: Technology, Codification and Application, Aluminium Structural Design, University of Naples "Federico II, No. 443, Springer, 2003, pp. 1-88, http://dx.doi.org/10.1007/978-3-7091-2794-0_1

[4] Lundberg, S.: Examples of Aluminium Applications in Various Environments Including Marine, Hydro Aluminum Profiler, 2011, pp. 3-20,.

[5] Aluminum Association (1998): Aluminum Alloy Selection and Applications, www.calm-aluminium.com.au/documents/aluminium-alloys.pdf.

[6] http://skyscrapercenter.com/building/tornado-tower/1677

[7] http://www.china-xiyi.com/product_index.php.

[8] Aluminum structural framing - building inspiration, Bosch Rexroth Corporation, 2009.

[9] Efthymiou, E., Cöcen, Ö.N, Ermolli, R.S.: Sustainable Aluminium Systems, Sustainability, 2010 (2), pp. 3100-3109, http://dx.doi.org/10.3390/su2093100

[10] Skejić, D., Boko, I., Torić, N.: Aluminium as a material for modern structures, GRAĐEVINAR, 67 (2015) 11, pp. 1075-1085, doi: 10.14256/JCE.1395.2015

[11] Vukašinović, V., Negevska-Cvetanovska, G., Kozinakov, D.: Uporedna analitička studija konstruktivnih elemenata od aluminijskih legura i čelika, Materijali i konstrukcije, 49 (2006) 1-2, pp. 25-33.

[12] Höglund, T.: TALAT Lecture 2301, Design of Members, Advanced Level, Royal Institute of Technology, Stockholm, EAA – European Aluminium Association, 2009, pp.19-30.

[13] Gabauer, W.: The determination of Uncertainties of Ramberg-Osgood Parameters (From a Tensile Test), Woest-Alpine Stahl Linz Gmbh, Issue 1, September 2000, pp. 1-16.

[14] Saga, M., Vaško, M., Malcho, M., Jadnačka, J.: Computational approach proposition for further processing of the fatigue curve, Applied and Computational Mechanics, 1 (2007), pp. 265-272.

[15] Höguld, T.,Tindal, Ph., UK Designers' Guide to Eurocode 9: Design of Aluminium Structures EN 1999-1-1 and -1-4, Annex E – analytical models for stress–strain relationship, The Institution of Civil Engineers (ICE) Publishing,Thomas Telford Limited, 2012, pp. 168-172.

[16] Su M.N., Young, B., Gardner, L.: Continuous Strength Method for Aluminium Alloy Structures, Advanced Materials Research, Vol. 742, Aug. 2013, pp. 70-75, http://dx.doi.org/10.4028/www.scientific.net/AMR.742.70

[17] Wei, D., Elgindi, M.B.M.: Finite Element Analysis of the Ramberg-Osgood Bar, American Journal of Computational Mathematics, 2013, 3, pp. 211-216, http://dx.doi.org/10.4236/ajcm.2013.33030

[18] Maljaars, J., Soetnes, F., Katgerman, L.: Constitutive Model for Aluminum Alloys Exposed to Fire Conditions, Metallurgical and Materials Transactios A, Volume 39A, April 2008, pp. 778-789, http://dx.doi.org/10.1007/s11661-008-9470-0

[19] Dokšanović, T., Markulak, D., Džeba, I.: State of the art review of the stability and welding of aluminium alloy elements, GRAĐEVINAR, 66 (2014) 2, pp. 115-125, doi: 10.14256/JCE.932.2013

[20] Morgenstern, C.: Kerbgrundkonzepte für die schwingfeste Auslegung von Aluminiumschweiß-verbindungen am Beispiel der naturharten Legierung AlMg4,5Mn (AW-5083) und der warmausgehärteten Legierung AlMgSi1 T6 (AW-6082 T6), Dissertation, Vom Fachbereich Maschinenbau an der Technische Universität Darmstadt, 2006, pp. 41-114.

[21] Wilson, C., Quillen, E.: Comparison of Elastic-Plastic Surface Crack Solutions, ASTM Workshop, Norfolk, May 23, 2008, www.astm.org/IMAGES03/E08Presentation_5.ppt

[22] Fourcade, T., Dalverny, O., Alexis, J., Seguineau, C., Desmarres, J.M.: Parametric identification of elastic-plastic constitutive laws using spherical indentation, http://oatao.univ-toulouse.fr/

[23] www.millproducts-alcoa.com, ALCOA Mill Products, Alloy 2024 Sheet and Plate.

[24] Benedyk, J.C.: International Temper Designation System for Wrought Aluminium Alloys: Part I-Strain Hardenable (H Temper) Aluminum Alloys, Light Metal Age, October 2009, pp. 26-30.

[25] Benedyk, J.C.: International Temper Designation System for Wrought Aluminium Alloys: Part II-Thermally Treated (T Temper) Aluminum Alloys, Light Metal Age, August 2010, pp.16-22.

[26] European Standards 10002-1, July 2001, Metallic materials-Tensile testing-Part 1: Method of Test at ambient temperature, Annex B, CEN 2001.

[27] Radović, Lj.: Deformacijsko ponašanje i karakteristike loma Al-Mg legura u svetlu međuzavisnosti sastav-tehnologija-struktura, Doktorska disertacija, Univerzitet u Kragujevcu, Fakultet tehničkih nauka Čačak, 2013, pp. 34-43.

[28] Hensel, A., Spittel, T.: Krafts und Arbeitsbedarf Bildsamer Formgebungverfaren, Deutscher Verlag Fur Grundstoff Industrie, Leipzig, 1978.

[29] Introduction the new STATEGRAPHICS CENTURION, http://www.statgraphics.com/download-trial

[30] Ashby, M., Jones, D.: Engineering Materials I, Third Edition, ELSEVIER Butterworth Heinemann, pp. 32-42.

[31] EN 1999-1-1 (2007): Eurocode 9: Design of aluminium structures - Part 1-1: General structural rules, European Committee for Standardization, 2009.

[32] ASTM B209 – 07: Standard Specification for Aluminum and Aluminum Alloy Sheet and Plate, American Society for Testing and Materials, 2007.

[33] ASM Handbook, 10th Edition, Volume 2: Properties & Selection - Nonferrous Alloys & Special-Purpose Materials, Materials Park, Ohio, 1990.

[34] Landolfo, R.: Cold-Formed Structures, Eurocode 9 -Part 1.4, Brussels, 2008, Dissemination of information workshop. http://eurocodes.jrc.ec.europa.eu/doc/WS2008/EN1999_8_Landolfo.pdf